AFOSR-TR-97 0405

REPORT DOCUMENTATION PAGE

Form Approved
OMB No. 0704-0188

1. AGENCY USE ONLY *(Leave blank)*	2. REPORT DATE	3. REPORT TYPE AND DATES COVERED
	September 1, 1997	FINAL REPORT 15 Jul 94 - 14 Jul 97

4. TITLE AND SUBTITLE
Ballistic Electron Emission Spectroscopy Study of Transport through Semiconductor Quantum Wells and Quantum Dots

5. FUNDING NUMBERS
61102F
2305/GS

6. AUTHOR(S)
Venkatesh Narayanamurti

7. PERFORMING ORGANIZATION NAME(S) AND ADDRESS(ES)
University of California, Santa Barbara CA 93106

8. PERFORMING ORGANIZATION REPORT NUMBER

9. SPONSORING/MONITORING AGENCY NAME(S) AND ADDRESS(ES)
Air Force Office of Scientific Research
AFOSR/NE
110 Duncan Avenue, Suite B115
Bolling AFB, DC 20332-0001

10. SPONSORING/MONITORING AGENCY REPORT NUMBER
F49620-94-1-0378

11. SUPPLEMENTARY NOTES

12a. DISTRIBUTION/AVAILABILITY STATEMENT
Distribution unlimited, approved for public release.

12b. DISTRIBUTION CODE

13. ABSTRACT *(Maximum 200 words)*

This report summarizes the development and use of Ballistic Electron Emission Microscopy (BEEM) for nondestructive, local characterization of semiconductor heterostructures under AFOSR grant No. F49620-94-1-0378. The technique has been applied for measuring heterojunction band offsets, for studying band structure effects in electron tunneling through double barrier resonant tunneling structures, and for imaging current flow through buried mesoscopic structures such as quantum dots (~10nm in size) and misfit dislocations 80nm below the surface. Monte Carlo simulations of the transport have also been performed.

The results suggest that BEEM is a powerful new low energy electron microscopy for materials physics study on the nm scale.

14. SUBJECT TERMS
Ballistic Electron Emission Spectroscopy, Ballistic Electron Emission Microscopy, BEEM

15. NUMBER OF PAGES

16. PRICE CODE

17. SECURITY CLASSIFICATION OF REPORT	18. SECURITY CLASSIFICATION OF THIS PAGE	19. SECURITY CLASSIFICATION OF ABSTRACT	20. LIMITATION OF ABSTRACT
UNCLASSIFIED	UNCLASSIFIED	UNCLASSIFIED	UL

Table of Contents

BALLISTIC ELECTRON EMISSION SPECTROSCOPY STUDY OF TRANSPORT THROUGH SEMICONDUCTOR QUANTUM WELLS AND QUANTUM DOTS

Principal Investigator: ***Venkatesh Narayanamurti***
Richard A. Auhll Professor and Dean of Engineering
Dept. of Electrical & Computer Engineering
University of California, Santa Barbara
Santa Barbara, California 93106
(805) 893-3141 Fax: (805) 893-8124
Internet: venky@engineering.ucsb.edu

Executive Summary

Ballistic Electron Emission Microscopy (BEEM) is a powerful new low energy electron microscopy in materials physics for nondestructive local characterization of semiconductor heterostructures. During the three year period of the AFOSR grant we have shown the power of this technique for (i) measuring heterojunction band offsets in planar semiconductor heterostructures in the prototypical $Al_xGa_{1-x}As$ system over the full composition range ($0 \leq x \leq 1$); and (ii) for studying band structure effects and quantum tunneling in double barrier resonant tunneling structures (DBRTS), also in the $Al_xGa_{1-x}As$ system. We have also shown the power of this technique for lateral imaging and spectroscopy with nm resolution for (iii) InAs self assembled quantum dots (SAD's) placed ~10mn below the surface; (iv) imaging $In_xGa_{1-x}As$/GaAs misfit dislocations buried 80mn below the surface; and finally (v) for measuring the variation in the heterojunction band offsets as a function of the order parameter in the GaInP/GaAs system.

The work reported above was performed primarily by J.J. O'Shea (Ph.D. 1997), T. Sajoto (Asst. Rsch. Engineer 1994-1995 and now at Applied Materials), and E.Y. Lee (Asst. Rsch Engineer 1995-1997 and now at Sandia National Laboratories, Livermore).

I. Introduction

Semiconductor heterostructures can be tailored to have desired electronic and photonic properties by careful bandgap engineering, control of the strain relief, and control of defects. Scanning-probe microscopy such as scanning-tunneling microscopy (STM) enables very high spatial resolution studies of the surfaces of structures of interest. Ballistic-electron-emission microscopy (BEEM) enables very high spatial resolution studies of thin films and their *buried* interfaces [1-2]. BEEM is an extension of STM and it is schematically shown below in Fig. 1.

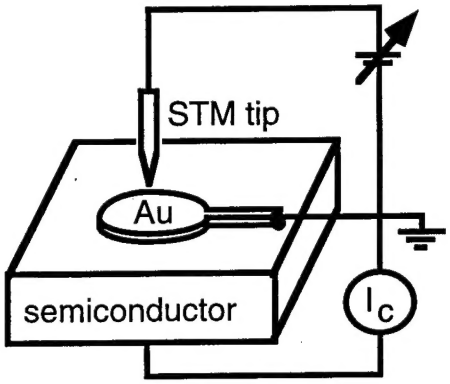

Fig. 1

In *our* typical BEEM experiment, a semiconductor heterostructure is capped with a thin layer (< about 100Å) of a metal (Au in our case), and the metal is grounded. There is typically no biasing of the metal with respect to the semiconductor.

As usual for STM, the tunnel current is maintained to be constant (typically a few nA) by a feedback loop that adjusts the tip-to-sample distance. In BEEM, an additional electrode is connected to the substrate to measure the current collected in the semiconductor, and this is called BEEM current I_c.

The STM tip is used to emit hot electrons or holes (depending on the tip-sample bias) of set energy over a point at the metal surface by quantum mechanical tunneling, by biasing the tip with respect to the grounded metal and by using piezoelectric scanners to move the tip laterally.

Fig. 2 shows an energy band diagram for BEEM. It can be seen that the STM tip functions as an emitter of hot electrons tunneling through vacuum into the metal base, because the tip is biased by V_t with respect to Au. The Au on the semiconductor forms a Schottky barrier of height eV_b, so an electron in Au must have at least this much energy to cross the Au-GaAs interface.

For the semiconductor heterostructure shown in Fig. 2, the semiconductor has a single barrier of $Al_xGa_{1-x}As$ between GaAs. For the electrons to be collected in the substrate, the energy must exceed the sum of the Schottky barrier height and band-offset ΔE_c of $Al_xGa_{1-x}As/GaAs$. Note that it is therefore possible to measure *local* heterojunction offsets in this

manner. Similarly, one can have a resonant tunneling barrier as the semiconductor heterostructure. In this case, BEEM threshold will be at the resonant transmission energy.

In BEEM imaging, the tip voltage and the tunnel current is held constant, and the location of the tip is varied and the BEEM current is measured. In spectroscopy, the STM tip is positioned over a point on the metal surface, and the tip bias is ramped. When the BEEM current is plotted as a function of V_t, the spectrum will show a threshold, which, depending on the semiconductor heterostructure under investigation, may be the Schottky barrier height, top of a single barrier, or a resonant transmission energy. The spectrum may also show additional higher thresholds if the semiconductor has satellite conduction bands or higher resonant transmission energies.

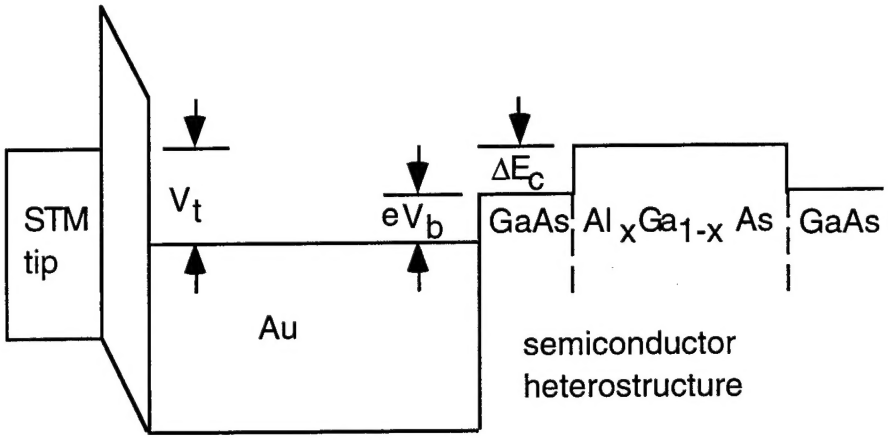

Fig. 2

Most BEEM studies have concentrated on the electronic structure at the metal-semiconductor interface (Schottky barrier formation) in the semiconductor such as Si, GaAs, and GaP [1,2]. A few studies have studied the semiconductor band structure [3,4]. Our work at University of California Santa Barbara (UCSB) has focused on the novel application of BEEM to study semiconductor heterostructures *buried spatially* beneath the Schottky barrier [5-10] and this will be described next.

II. Summary of UCSB BEEM work under AFOSR Grant

At UCSB we have developed two state-of-the-art variable temperature (currently 77K to 300K) BEEM instruments capable of providing stable data over long periods of time. These, combined with the ready access to large numbers of MBE and MOCVD grown samples, has enabled us to establish BEEM as a powerful spectroscopic *and* microscopic tool for probing compound semiconductor heterostructures *buried spatially* beneath the Schottky barrier. Below, we show the three kinds of structures that we have investigated.

Fig. 3 shows schematic diagrams for (a) a Au/GaAs Schottky barrier; (b) a single barrier/well structure; and (c) a double barrier resonant tunneling structure placed beneath the Au/GaAs Schottky barrier. Such structures have the advantage that the Au/GaAs interface is invariant and

allows a systematic comparison to be made as one varies the nature of the heterostructure and alloy composition.

It is important to note that all our samples were grown at UCSB by MBE and MOCVD, and that Au was evaporated after passivation of the GaAs surface by NH_4OH etch. Due to the epitaxial quality of our MBE and MOCVD grown GaAs, the Schottky barrier height for Au/GaAs is spatially uniform. By BEEM, we measure it to be 0.92±0.03eV (for n-type GaAs(001)) at 300K, and this value agrees excellently with values by other techniques such as I-V, C-V, and internal photoemission. The exceptional uniformity of the Au-GaAs interface allows us characterization of features *below* this interface by BEEM.

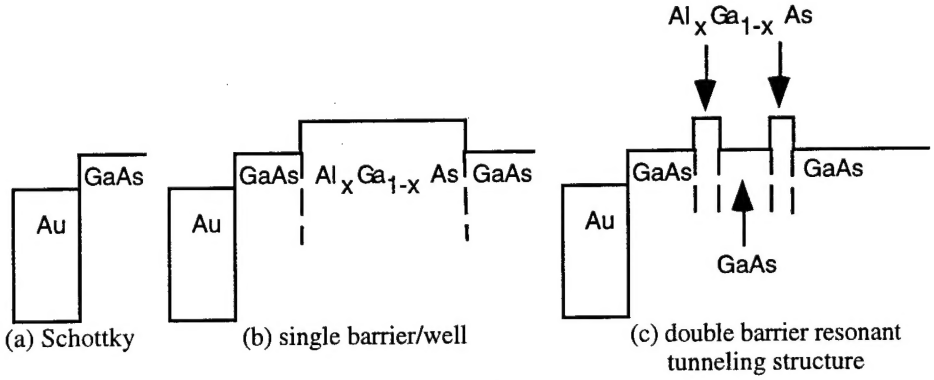

Fig. 3

II.1. Single barrier of $Al_xGa_{1-x}As$/GaAs: band-offset vs. Al concentration

For the single barrier case (Fig. 3(b)), we have varied the height of the $Al_xGa_{1-x}As$ barrier by systematically varying the Al composition [5]. The barrier thickness was 100 Å and the GaAs capping layer was also 100 Å. We used Be delta doping in the GaAs buffer layer to flatten the built-in field in our heterostructures. (Poisson and Schrödinger equations were simultaneously solved using a program to calculate the required dopant sheet concentration.)

In Fig. 4, we show the BEEM spectra for five Al compositions (0, 0.11, 0.21, 0.32, 0.42). The BEEM thresholds indicated above were gotten by fitting the spectra to the Bell-Kaiser theory [1]. The offsets deduced from this work are in excellent agreement with offsets known for this system. Alternative theories or fit procedures give the same thresholds within 30 meV. Knowing the Schottky barrier height of Au/GaAs, we can directly derive the band-offsets for $Al_XGa_{1-x}As$/GaAs by subtracting the Schottky barrier height from the measured BEEM threshold.

Figure 5 shows the initial onsets (ΔE_C) relative to GaAs as a function of Al composition x for the Direct regime ($0 \leq x \leq .42$) for room temperature (RT) and 77K. Figure 6 shows a detailed fit to the BEEM spectra for GaAs. The theoretical model developed by Bell and Kaiser [2] was used to fit the data. The fits show additional thresholds due to electron transmission into higher valleys L and X besides Γ.

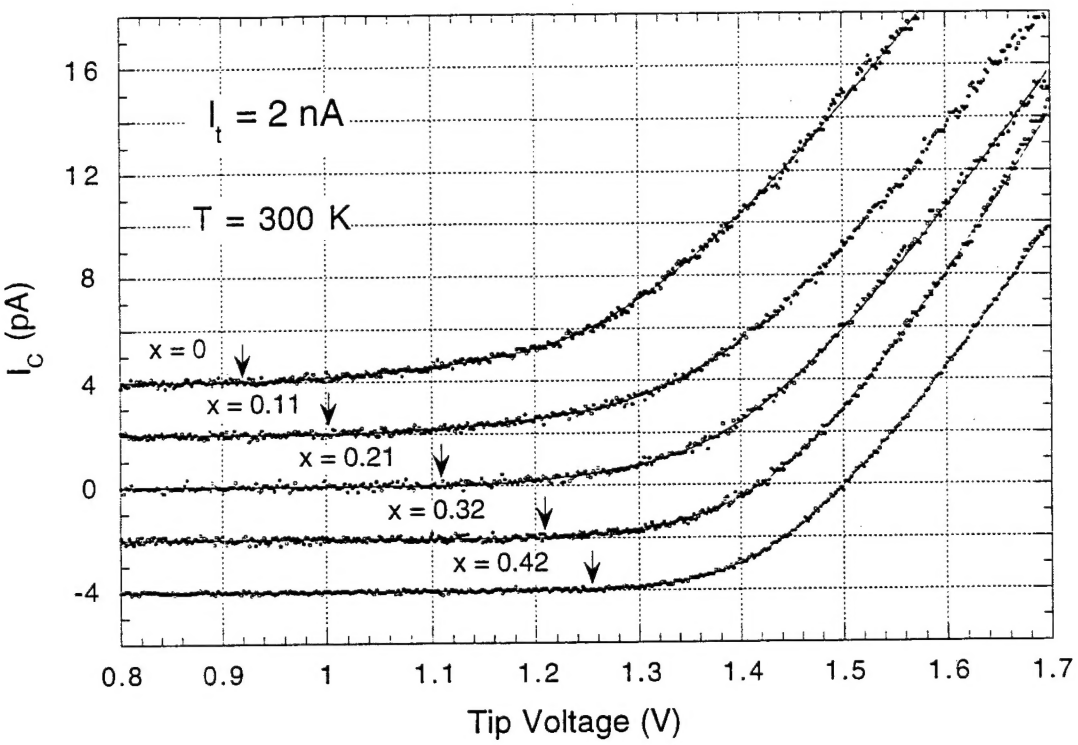

Fig. 4

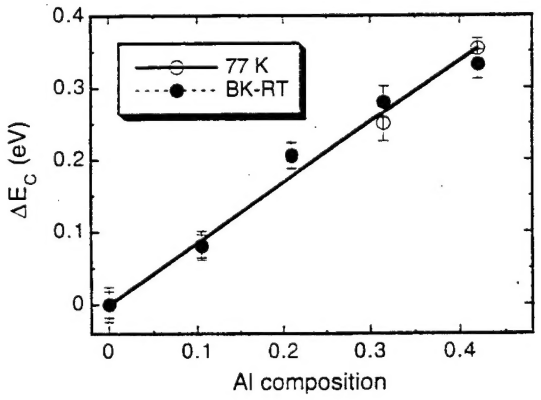

Figure 5. RT and 77K GaAs/$Al_xGa_{1-x}As$ conduction-band offsets (points) measured by BEEM. Linear fits (lines) at both temperatures give ΔE_C=(0.84 eV)x, or a fractional band offset of $Q_C=\Delta E_C/\Delta E_g$=0.68. The linear curve fits and some data points are overlapping.

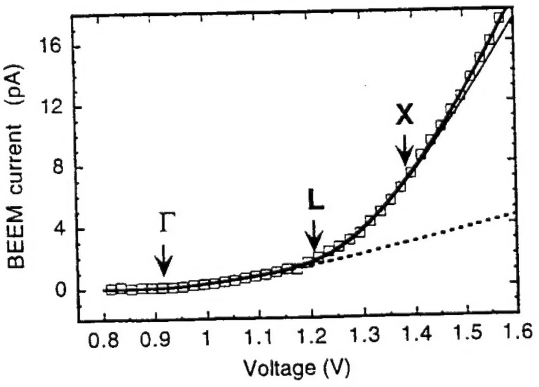

Figure 6. Typical RT BEEM spectra (points) for AuGaAs ("AL0") sample. Least squares fits (lines) to the BK model included current injected into the GaAs Γ, L, and X bands. Thresholds of 0.92, 1.21, and 1.38 eV are found in good agreement with the expected interband energies.

By systematic studies as a function of Al composition x we have studied the effects on the band structure in the $Al_xGa_{1-x}As/GaAs$ system. Figure 7 provides a detailed summary of the results.

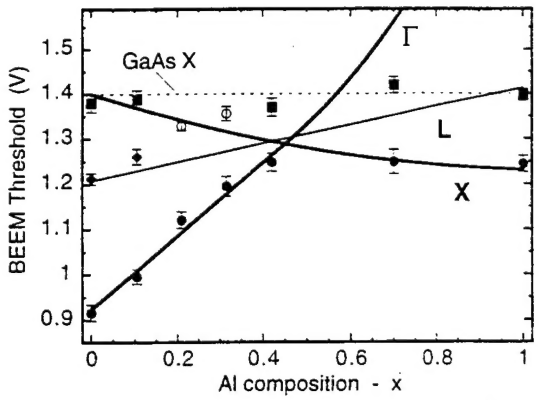

Figure 7. Summary of RT BEEM thresholds (point) for 100Å $Al_xGa_{1-x}As/GaAs$ single-barrier heterostructures. Lines show the composition dependence of band minima assuming a linear valence-band offset, $\Delta E_V=(0.44\,eV)x$. Good agreement with the $Al_xGa_{1-x}As$ absolute conduction-band minimum (filled circles), the $Al_xGa_{1-x}As$ L point (filled diamonds) and the GaAs X point (filled squares) is found. For x=0.21 and 0.32, the second BEEM threshold (open circles) represents an average of the L and X band contributions.

These data represent the most systematic study of band offset and band structure effects using BEEM. They resulted in a substantive PhD thesis and a major publication.

II.2. Single barrier of $Ga_xIn_{1-x}P/GaAs$: band-offset vs. order parameter

A particularly topical interesting system for BEEM is the $Ga_xIn_{1-x}P/GaAs$ system, which is known to exhibit ordering, i.e. the Ga and In atoms stack alternately in an ordered instead of a random array. This system has potential applications for heterojunction bipolar transistors, visible LED's, and solar cells. Yet, such fundamental parameters as heterojunction band-offsets are not well understood. Experimentally, values of conduction band offsets ranging from 30 to 390 meV have been reported [11]. We have recently measured the $Ga_{0.52}In_{0.48}P/GaAs$ conduction band offsets and given the first, clear evidence that they depend directly on the degree of ordering in $Ga_xIn_{1-x}P$ [9] and provide a cogent explanation for the previously observed large variations in band offsets.

For our BEEM experiment, we grew simultaneously by MOCVD ~1μm of undoped $Ga_{0.52}In_{0.48}P$ on two different n^+-GaAs(001) substrates, one misoriented from (001) by 6° to (111)A and the other misoriented by 6° to (111)B. Let us refer to these as samples A and B. Different substrate misorientations are expected to induce different degree of ordering in the $Ga_{0.52}In_{0.48}P$ epilayers. As usual for us, additional 50 Å of GaAs capping layer and ~80 Å of Au were also deposited to make a single barrier structure of the kind shown in Fig. 3(b).

Photoluminescence measurements showed energy band gaps of 1.97 and 1.89 eV at 2K for samples A and B, respectively, and this implied order parameters η's of 0.3 and 0.5 according to theory [12]. Fig. 8 shows the BEEM spectra from each of these samples. BEEM thresholds of 1.052±0.025 and 1.001±0.021 V can be seen. Since the Au/GaAs Schottky barrier height is 0.92eV and we expect 0.016eV voltage drop across the 50Å GaAs capping layer due to the electric field in the depletion region, we *directly* get $Ga_{0.52}In_{0.48}P$/GaAs band-offsets of 1.052-0.92+0.021=0.153eV for sample A (η=0.3) and 1.001-0.92+0.016=0.097eV for sample B (η=0.6).

Furthermore, we observed ridge structures, shown in Fig. 9 (bias of 1.7 V and tunnel current of 1nA), in the topography and accompanying contrast in the BEEM image which may correspond to localized ordered domains in the GaInP or to spatial variation of the Ga concentration. ~20 meV spatial variation of BEEM threshold was observed across these structures. These measurements show the power of BEEM to provide new information on electronic transport on a *local* scale, not possible by any other technique.

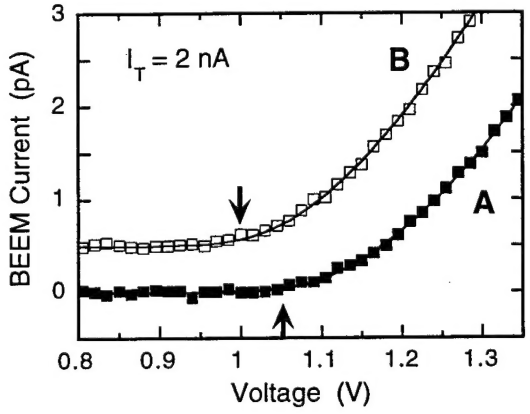

Fig. 8: BEEM spectra taken on samples A and B

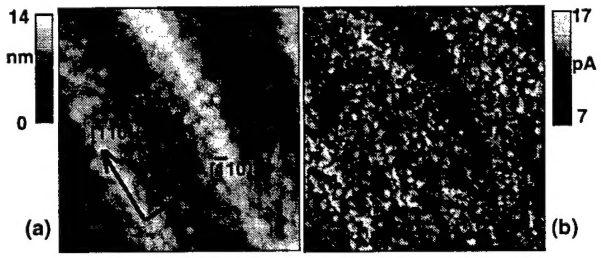

Fig. 9: simultaneously taken (a) STM and (b) BEEM images from sample B

II.3. Single well of $In_xGa_{1-x}As$/GaAs: imaging and spectroscopy of misfit dislocations at the $In_xGa_{1-x}As$/GaAs interface

$In_xGa_{1-x}As$/GaAs heterostructures are widely used in heterojunction bipolar transistors and lasers. The study of dislocations in such structures by cathodoluminescence (CL) and transmission electron microscopy (TEM) is technologically important, and yet detailed understanding of their nature remains elusive.

We have recently done BEEM imaging and *spatially resolved* spectroscopy of $In_xGa_{1-x}As$/GaAs misfit dislocations 800 Å below the surface [8]. Majority-carrier scattering by a fraction of misfit dislocations was seen to locally reduce the BEEM current and to give logarithmic spatial dependence, which suggests charging of the dislocation cores. This is the first time that a defect

in a semiconductor heterostructure has been identified by BEEM and transport through it has been energetically resolved.

Our sample consisted of single well (see Fig. 3(b)) of 600Å thick $In_{0.25}Ga_{0.75}As$ on GaAs(001) capped with 100Å of GaAs and 100Å of Au overlayer. The $In_{0.25}Ga_{0.75}As$ thickness exceeded the critical thickness and hence misfit dislocations formed at the bottom $In_{0.25}Ga_{0.75}As$/GaAs interface to relieve strain.

Fig. 10 shows a pair of simultaneously taken empty state STM image and BEEM image, which captured three dislocations running along the [110] direction. The images were taken at tip-sample bias of –1.5V and tunnel current of 4 nA. The STM image shows three faint protrusions ~1nm high and ~500Å wide (FWHM), due to the underlying cross-hatch pattern, which is caused by the dislocation core. (The details cross-hatch pattern formation is not well understood.) The small features in Fig. 10(a) are Au grains 100-200 Å in diameter .

The corresponding BEEM image shows three dark lines near the underlying cross-hatch patterns, but *not* at the same locations. These are misfit dislocations at the $In_{0.25}Ga_{0.75}As$/GaAs interface, and the lateral displacement of the dislocations from the cross-hatch pattern is actually *expected*, since the cross-hatch patterns originate in part from lattice slips caused by the dislocations and the dislocations glide on {111}, which forms 57.4° from [001].

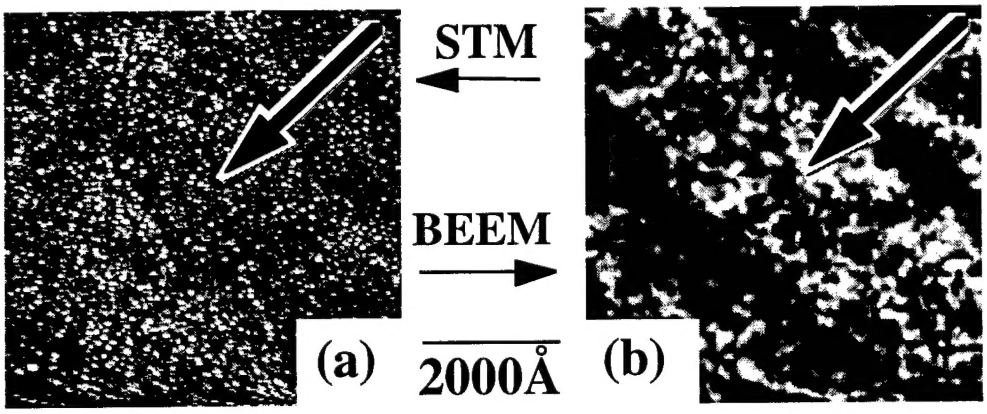

(a) STM image of 6000 ¥ 6000Å2 area gray scale over 80 Å

(b) simultaneously taken BEEM image gray scale from 4 to 8 pA

Fig. 10

Fig. 11(a) shows average of cross sections parallel to the arrows shown in Fig. 10. A clear offset of ~500 Å can be seen between the center of the surface protrusion due to the cross-hatch pattern and the center of dip in the BEEM current. The good fits to the curves are to Gaussian and to logarithmic functions, respectively, which suggest charging or strain field scattering of hot electrons from the misfit dislocations.

In Fig. 11(b) we show spatially resolved BEEM spectroscopy near (filled circle) and away (empty circle) from dislocation. The tunnel current was 4 nA and the inset shows the difference spectra normalized by the average spectrum. It can be seen that the BEEM contrast is largest at low energies, and that significant contrast exist below the band gap energy of $In_{0.25}Ga_{0.75}As$. This fact demonstrates that BEEM is fundamentally different from cathodoluminescence or electron-beam-induced current, both of which require band gap excitation of thousands of electron-hole pairs. Clearly, BEEM is a new form of *low* energy electron microscopy capable of providing *local* spectroscopic information of objects *buried* hundreds of Ångstroms below the surface.

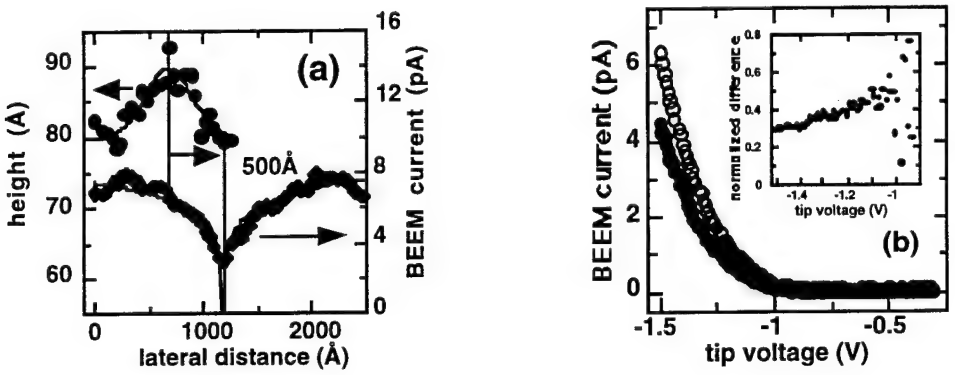

(a) STM and BEEM cross sections (b) BEEM spectra

Fig. 11

II.4. Double barrier resonant tunneling structure

For our study of double barrier resonant tunneling structure (DBRTS), we made 23 Å thick $Al_{0.42}Ga_{0.58}As$ double barriers sandwiching a 17 Å thick GaAs quantum well (see Fig. 3(c)). As always, there was a 100 Å thick GaAs cap. In designing this structure, we wanted the $Al_{0.42}Ga_{0.58}As$ barriers thin enough to allow significant transmission and the GaAs quantum well thin enough to push up the resonant transmission energies, for them to be readily observable. Fig. 12 shows the second derivative of the BEEM current as a function of the tip voltage. Recent theoretical work by Smith and Kogan [13] has shown that the second derivative of the BEEM current is approximately proportional to the transmission probability across buried semiconductor heterostructures.

Six spectra taken at various temperatures between 300K and 77K are shown in Fig. 12. The spectra are displaced vertically for clarity, and the one at 77K was scaled by 1/5 for ease of viewing. The peaks correspond to resonant transmission energies through DBRTS. There is significant temperature dependence arising from change of the band gaps, phonon scattering, and thermal broadening. Detailed study of the derivatives clearly showed the effects of the electronic band structure and resonant tunneling [6], and has been discussed in detail by us in a recent publication [7].

These measurements have shown the power of BEEM to measure band-offsets and to study tunneling and transport in quantum heterostructures. Since the structures were grown to be spatially uniform, the corresponding BEEM images were quite uniform.

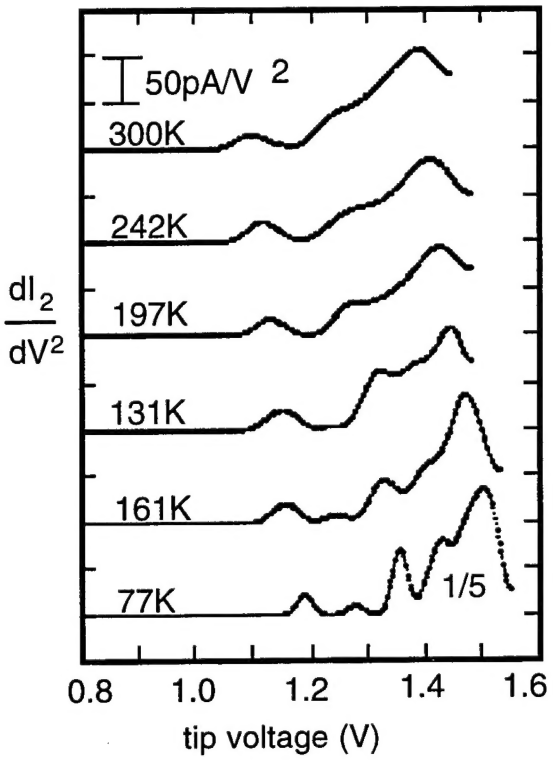

Fig. 12

II.5. InAs quantum dots: resonant tunneling through 0-D quantum states

We have recently succeeded in imaging buried quantum dots by BEEM for the first time. We have also done BEEM spectroscopy over single quantum dots ~200 Å in diameter and 30 Å tall, by exploiting the lateral resolution of BEEM [10]. One may imagine the following two situations.

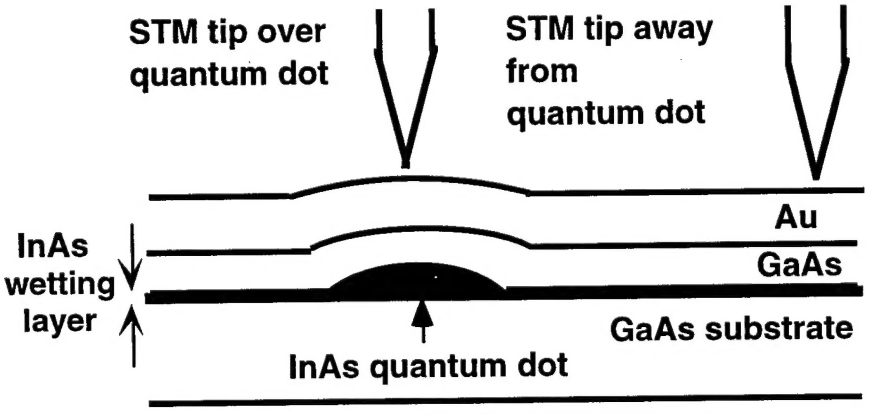

Fig. 13

The size of the quantum dots varies as a function of the kinetics and the thermodynamics during growth, but, for the InAs quantum dots grown for our work, they tends to spontaneously form ("self-assemble") to be approximately ~30Å thick and ~200Å in diameter, under certain growth conditions [14]. In our case, 1.5 monolayers of In were deposited at 530° onto 300 Å of undoped GaAs buffer on n^+-GaAs(001) to form InAs quantum dots. InAs wetting layer a few monolayers thick is believed to exist everywhere, and the spacing between the dots depend sensitively on the amount of In deposited. Previous electrical characterizations such as C-V measurements were done on ensembles of hundreds or thousands of dots. With BEEM we were able to study the electrical transport through *single* quantum dots.

The quantum dots and the wetting layer form quantum wells bounded on both sides by GaAs, and there are bound states associated with these quantum dots, which are analogous to artificial atoms. We can locate the quantum dots by STM and tunnel into the bound states via resonant tunneling to directly probe the bound states and resonant transmission energies by BEEM (see Fig. 13).

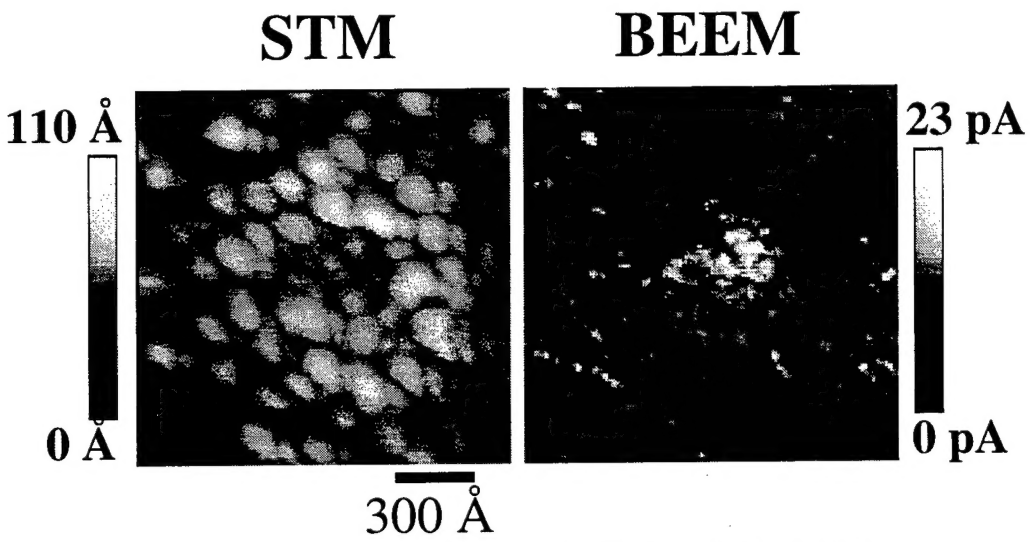

(a) STM image of a quantum dot (b) simultaneously taken BEEM image

Fig. 14

Fig. 14 shows simultaneously taken STM and BEEM images, in which the BEEM image shows enhanced BEEM current through a quantum dot *buried* beneath the surface (in this case, by 50Å GaAs cap and 85Å Au overlayer). The STM image shows an elongated island ~1000Å in diameter ~50Å in height. The InAs quantum dot is buried near the center of the island, where there is a slight depression. The island formation is driven by strain of 7.16% lattice mismatch between InAs and GaAs, but the details of the phenomenon is not well understood. Au grains 100-200Å in diameter can be seen to uniformly cover the entire area. The corresponding BEEM image clearly shows larger BEEM current over the quantum dot *with nm spatial resolution*..

Spatially resolved BEEM spectroscopy was also done on top of the quantum dot and away from it, and it is shown in Fig. 15. The arrows and the solid line are fits to the Bell-Kaiser theory [1], and reflect strain induced change of the GaAs capping layer Γ and L conduction band minima. *In addition*, BEEM current thresholds at 0.62 and 0.72V can be seen, and these correspond to resonant tunneling (see Fig. 3(c)) through 0-D quantum dots states of a *single* quantum dot. The measured values agree well with ensemble average over thousands of dots gotten by C-V measurement [15].

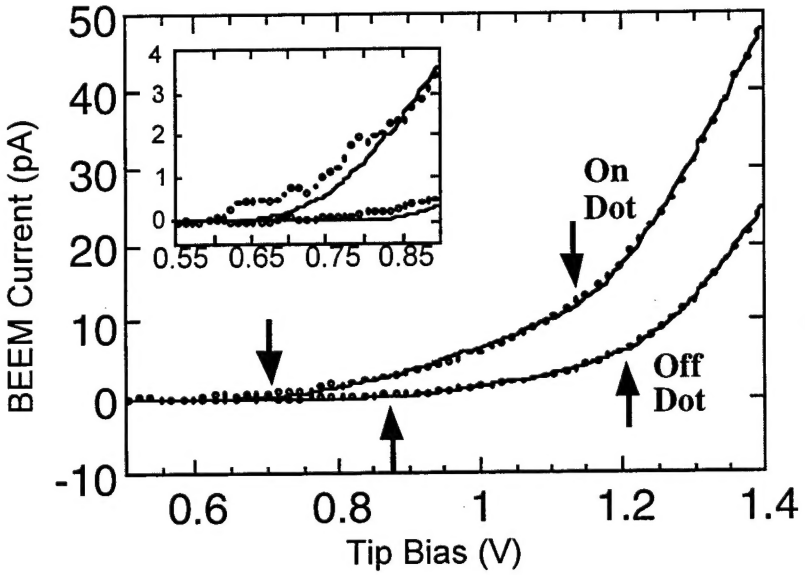

Fig. 15: spatially resolved spectroscopy over a *single* quantum dot

II.6. Monte Carlo simulation

In order to get a quantitative understanding of BEEM transport, particularly sub-surface BEEM imaging, we performed [16] Monte Carlo simulations for spatially resolved imaging and spectroscopy of buried quantum objects. To determine the spatial resolution and the energy resolution of BEEM for buried mesoscopic structures, the current fluxes and the electron normal wave vector are obtained as a function of the depth from the Au-GaAs interfaces. The BEEM current cross-sections and the spatially resolved BEEM spectra on and off these structures are calculated in order to study their dependence on the depth and the scanning tunneling microscope tip-to-sample bias. The results show that Γ electrons roughly 0.5V above the band edge are truly ballistic and that the spatial resolution is of the order of the depth, and confirm the usefulness of BEEM for imaging mesoscopic structures, heretofore not possible.

III. Conclusion

Under the AFOSR grant we have developed and shown the power of a new form of low energy electron microscopy, namely BEEM, for probing the transport characteristics of buried mesoscopic objects and defects in a regime (10 to 100nm) not heretofore possible. This technique can now

be applied for physical characterization of new semiconductor materials of importance to the emerging field of nanoelectronics and nanotechnology.

IV. Bibliography

[1] Kaiser and L. D. Bell, *Phys. Rev. Lett.* **60**, 1406 (1988); *ibid.* 61, 2368 (1988).

[2] For a recent review, see L. Douglas Bell and William J. Kaiser, *Annu. Rev. Mater. Sci.* **26**, 189(1996).

[3] For the latest progress on BEEM, see the *Fifth Annual Workshop on Ballistic Electron Emission Microscopy Conference Proceedings*, 24 January 1994, Mohonk, NY, chaired by V. Narayanamurti; H. Sirringhaus, E. Y. Lee, and H. von Känel, *Phys. Rev. Lett.* **73**, 577(1994); E. Y. Lee, H. Sirringhaus, U. Kafader, and H. von Känel, *Phys. Rev. B* **52**, 1816 (1995) and references therein.

[4] W. J. Kaiser, M. H. Hecht, L. D. Bell, F. J. Grunthaner, J. K. Liu, and L. C. Davis, *Phys. Rev. B* **48**, 18324 (1993); R. Ludeke, *Phys. Rev. Lett.* **70**, 214(1993).

[5] J. J. O'Shea, T. Sajoto, S. Bhargava, D. Leonard, M. A. Chin, and V. Narayanamurti, *J. Vac. Sci. Technol. B* **12**, 2625 (1994); and J. J. O'Shea *et al.*, *Phys. Rev. B* **56** (3) 2026 (1997) and Ph.D. Thesis, University of California..

[6] T. Sajoto, J. J. O'Shea, S. Bhargava, D. Leonard, M. A. Chin, and V. Narayanamurti, *Phys. Rev. Lett.* **74**, 3427 (1995).

[7] V. Narayanamurti, *SPIE Proceedings* **2397**, 125 (1995), see also *Festkörperprobleme/Advances in Solid State Physics* **35**, 243-256, 1995

[8] E. Y. Lee, S. Bhargava, K. J. Pond, K. Luo, M. A. Chin, and V. Narayanamurti, *Appl. Phys. Lett.* **69**(7), 940(1996).

[9] J. J. O'Shea, C. M. Reaves, S. P. DenBaars, M. A. Chin, and V. Narayanamurti, *Appl. Phys. Lett.* **69** (20), 3022 (1996).

[10] M. E. Rubin, G. Medeiros-Ribeiro, J. J. O'Shea, E. Y. Lee, P. M. Petroff, and V. Narayanamurti, *Phys. Rev. Lett.* **77**. 5268 (1996).

[11] S. L. Feng, *et. al. Semicond. Sci. Technol.* **8**, 2092(1993) and references therein.

[12] S.-H. Wei, A. Zunger, *Appl. Phys. Lett.* **56**, 662(1990); K. A. Mäder and A. Zunger, *Appl. Phys. Lett.* **64**, 2882(1994).

[13] D. A. Smith and Sh. M. Kogan (*Physical Review B* in press).

[14] D. Leonard, M. Krishnamurthy, C. M. Reaves, S. P. DenBaars, and P. M. Petroff, *Appl. Phys. Lett.* **63**, 3203 (1993).

[15] H. Drexler, D. Leonard, W. Hansen, J. P. Kotthaus, and P. M. Petroff, *Phys. Rev. Lett.* **73**, 2252(1994).

[16] E.Y. Lee, V. Narayanamurti, and D.L. Smith, *Phys. Rev.* **55**, R16033 (1997).